JOURNAL OF APPLIED ELECTROCHEMISTRY **28** (1998) 227–236

# Fundamentals of electrosorption on activated carbon for wastewater treatment of industrial effluents*

A. BÁN, A. SCHÄFER, H. WENDT

*Institut für Chemische Technologie, TU Darmstadt, Petersenstrasse 20, D-64287 Darmstadt, Germany*

Received 13 January 1997; revised 20 April 1997

The potential of electroadsorption/desorption on activated carbon for waste water treatment of industrial effluents is studied. Adsorption isotherms of hydrophobic differently charged model substances on activated carbon were measured in order to obtain specific information about the influence of the charge ($+1, -1$ and 0) on the adsorbability of comparable, aromatic species and the influence of the bed potential on the adsorption equilibria. In all these cases the adsorption equilibria show a dependence on applied potential in electrolyte of approximately 1 M ionic strength. With electrosorption from aqueous solution, a fivefold enhancement of the concentration in one potential controlled adsorption/desorption cycle is achievable. The use of the solvent methanol instead of water for desorption allows for a concentration enhancement by a factor of hundred in the desorptive step. The adsorption capacity of the activated carbon changes only slightly with cycle number. Two cell designs for the performance of potential controlled adsorption/desorption cycles on the large scale are discussed.

Keywords: *wastewater treatment*, *electrosorption*, *activated carbon*, *electrochemical process*, *adsorber bed*, *regeneration*

## 1. Introduction

Industrial effluents from chemical production often contain small amounts of toxic and hardly degradable organic substances, together with a high electrolyte concentration. Adsorption on activated carbon is often used as a powerful cleaning step for waste water with lower pollutant concentration. Generally, the loaded carbon is regenerated by the manufacturer by heating to relative high temperatures, which is a costly procedure (1000 DM $m^{-3}$ or up to 70% of the operating costs [1, 2]). Utilizing potential controlled adsorption/desorption (electrosorption) would allow for increased adsorption capacity on one hand and *in situ* regeneration of the adsorber bed on the other hand. Further it could establish a method of pollutant reconcentration. A possible electrochemical degradation of organic pollutants in the adsorbed state is also of industrial interest. Another application of electrosorption on activated carbon could be the enrichment of valuable chemical or biogenic substances. The electrosorption of inorganic and organic molecules and ions on metal interfaces is a relatively well understood phenomenon, in particular with respect to the mercury/aqueous interface [3–5].

The structure of a metal or activated carbon surface/aqueous electrolyte interface is schematically depicted in Fig. 1(a) for the case of zero charge density at the electrode surface. The surface is mainly covered by adsorbed water dipoles. Other surfactive ions or molecules from the solution are also possibly contact-adsorbed. While charging the electrode, the charge on the electrode is compensated by ionic countercharges at the electrolyte side of the interface. This compensation can occur by contact adsorption of ions as shown in Fig. 1(b) and/or by an accumulation of counterions in the outer Helmholtz plane and the diffuse (Gouy–Chapman) layer. The water dipoles tend to align with the electric field.

Due to the coulombic interaction, adsorptive equilibria of positively, negatively and uncharged particles are specifically dependent on the electrode charge. Figure 2 shows schematically the polarization dependence of the surface loading related to the potential of zero charge, $E_{pzc}$, with an assumed constant concentration of the adsorbed material in the electrolyte.

Potentials anodic to $E_{pzc}$ decrease the amount of cations adsorbed at the surface and inversely increase the amount of adsorbed anions. Uncharged molecules are most strongly adsorbed at, and close to, the potential of zero charge, $E_{pzc}$. They become desorbed at increasingly higher cathodic or anodic potentials due to increasingly higher coulombic interactions between the electrode charge and the solvent dipoles. The latter tend to displace uncharged adsorbed species the higher the charge density on the electrode.

For the nonpolarizable mercury electrode, a lot of work has been done to give a more detailed insight into the different attractive and repulsive forces and adsorption energies in relation to the electric poten-

---

[*] This paper was presented at the Fourth European Symposium on Electrochemical Engineering, Prague, 28–30 August 1996.

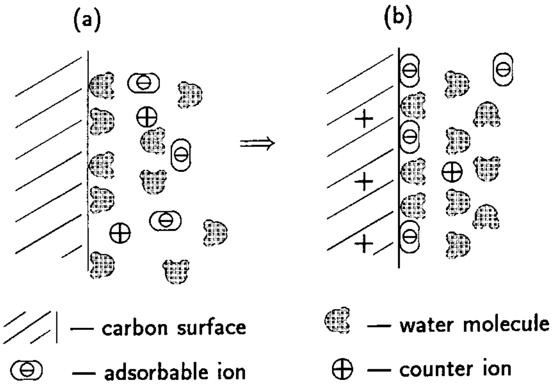

Fig. 1. Schematical representation of the interphase region of an uncharged (a) and charged (b) activated carbon surface.

tial [4] and the charge density [5]. However, these results cannot be transferred to the activated carbon electrode because of its surface groups, its energetically heterogeneous surface and the complicated potential distribution in the granules.

Work has also been done on carbon electrodes. Alkire and Eisinger [6, 7] presented adsorption isotherms of organic compounds at nonporous glassy carbon and graphite and developed a mathematic model for the mass and current distribution in a flow-through adsorber.

Further thermodynamic adsorption data are published, for example for the adsorption of quinones (Strohl and Dunlap [8]), *n*-hexanol, cyclohexanol, nitrobenzene (Khabalov *et al.* [9]) or complex molecules like rhodamine B, tryptophan (Mayne and Shackleton [10]) etc. on modified graphite electrodes or on activated carbon electrodes for example phenol (McGuire *et al.* [11], Narbaitz and Cen [12]), benzoic acid (Khabalov *et al.* [13], Novikova *et al.* [14]), *o*-nitrophenol (Chue *et al.* [15]), chloroform (Bonnecaze *et al.* [16]), caprolactam (Lisitskaya *et al.* [17]), ethanol, ethylacetate (Tarkovskaya *et al.* [18]), *n*-alcohols (Zabasajja and Savinell [19]) etc.

Abramov [20], Besenhard *et al.* [21] and Reed and Nonavinakere [22] used activated carbon for ion exchange of inorganic ions. Grevillot [23] calculated the potential and mass distribution in a packed bed and developed a theoretical model for the electroad- and desorption kinetics. Kastening [24] and Kastening

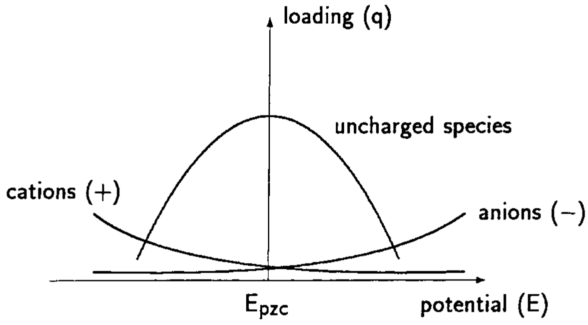

Fig. 2. Schematic presentation of the potential dependence of the loading, *s*, for differently charged molecules/ions [3].

and Müller [25] investigated the double layer of activated carbon and the adsorptive behaviour of inorganic ions. He found that the high capacity of his activated carbon samples ($C = 100\text{–}120\,\mathrm{F\,g^{-1}}$) is due to the double layer capacity and any redox processes at the carbon surface are negligible. He also showed that specific adsorption of inorganic ions occur, leading to an increase/decrease of the potential of zero charge, $E_{\mathrm{pzc}}$.

It is the aim of this work to investigate electrosorption equilibria of a number of model substances on a commercially available activated carbon to obtain a solid basis for estimating the technical potential of electrosorption for the purification of industrial waste waters. The results are confined to data obtained with one particular activated carbon quality which is assumed to exhibit the typical qualities of activated carbons currently used for waste water treatment and electrolytes of approximate 1 M ionic strength.

As a typical example of commercially available activated carbons, Norit ROW 0,8 Supra of Norit Deutschland was chosen as its properties are representative of a number of activated carbons which had been investigated [26].

## 2. Experimental details

Measurements of potential controlled adsorption isotherms and adsorption kinetics were carried out in a closed loop, depicted schematically in Fig. 3. A reservoir, a gear pump, the cell (fully detailed in Fig. 4) and an u.v. spectrometer constitute the loop. The circulating electrolyte was 0.1 M KCl. The po-

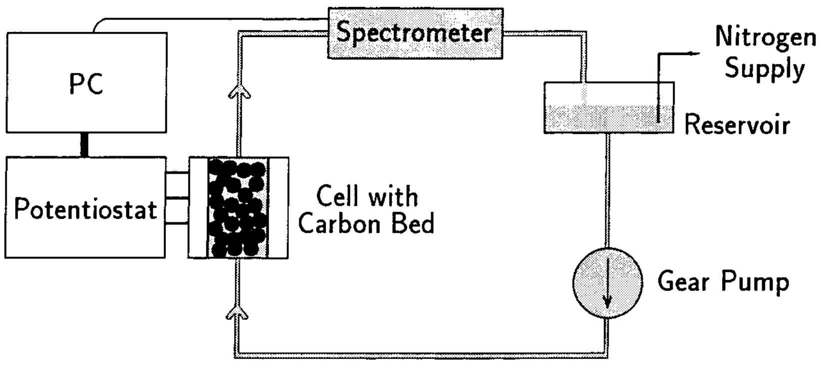

Fig. 3. Electrolyte loop comprising a reservoir, a gear pump, the cell and an u.v. spectrometer.

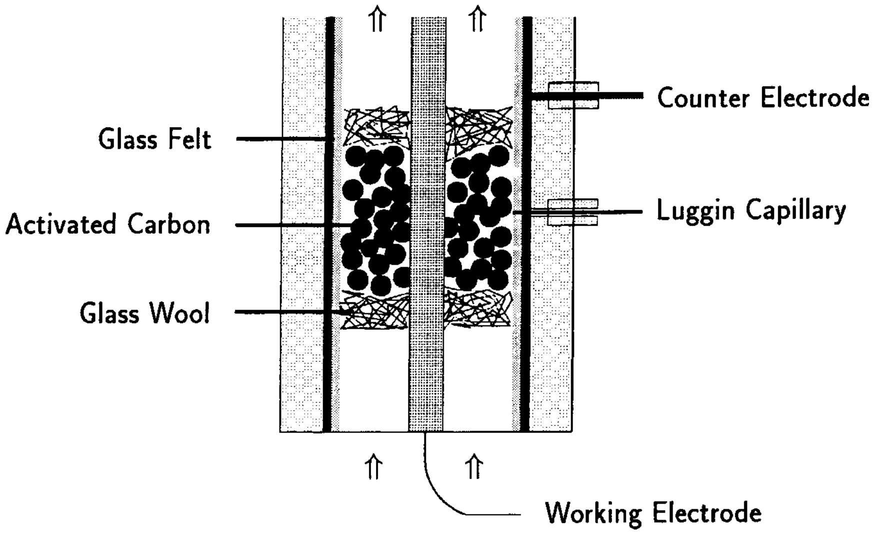

Fig. 4. Schematic of the cylindrical activated carbon packed bed cell.

tential of the cell was controlled by a potentiostat, connected to a PC-based data acquisition system, as well as the spectrometer for monitoring concentration, electrode potential and electrode current against time. Materials in contact with the electrolyte were only platinized titanium, PTFE and glass.

The cell (Fig. 4) was made of Teflon (PTFE) and contained about 0.5 g of granular activated carbon. Norit ROW 0,8 Supra from Norit Deutschland with a BET surface of $950\,\mathrm{m}^2\,\mathrm{g}^{-1}$ was used in all experiments; this was extracted for two weeks in a soxhlet apparatus with conc. HCl and was further purified by subsequent washing with water. Typical dimensions of the cylindrical carbon granules were 0.8 mm × 3 mm. The packed bed of active carbon was contacted with a platinized titanium cylinder in the centre of the cell and surrounded by the counter electrode, a silver plate. A glass felt was used in order to insulate electronically the carbon bed and the counter electrode. The reference electrode was connected to the carbon bed via a Luggin capillary.

The chosen model substances were methylquinolinium chloride (as a singly charged aromatic cation), benzyl alcohol (as an uncharged aromatic species), naphthalenesulfonic acid potassium salt and naphthoic acid potassium salt (as singly charged aromatic anions), because they are u.v. detectable, stable over a wide potential range and moderately water soluble.

For an accelerated retrieval of the equilibrium data, a second cell type was constructed, as shown in Fig. 5. The activated carbon (125 mg) was located on a perforated plate. The reference electrode was an oxidized silver wire in a Teflon tube, filled with saturated KCl solution and closed with a porous polyphenylensulfide felt. The solution (10 ml) was agitated with a magnetic stirrer. 25 of these minicells were operated in parallel at different electrode potentials. Experiments made with this cell type were in good agreement with those obtained in the loop shown in Fig. 3.

The same equipment (with 125 mg activated carbon and 10 ml of 0.1 M KCl solution) was also used for acidity measurements of the activated carbon, determining the dependence between imposed potential and pH value.

Several buffers were added to the solution to investigate the effect of the pH on adsorption. For $\mathrm{pH} < 1$, 0.5 M HCl was added, for pH 7 0.15 M $K_2HPO_4$ and 0.15 M $KH_2PO_4$ was added. For pH 9, it was 0.15 M $K_2B_4O_7$ and 0.15 M $KHB_4O_7$, for pH 12, 0.15 M $K_2HPO_4$ and 0.15 M $K_3PO_4$ and for pH 14, 0.5 M KOH was added.

The potential of zero charge $E_{\mathrm{pzc}}$ of the activated carbon was measured by taking a degassed sample of

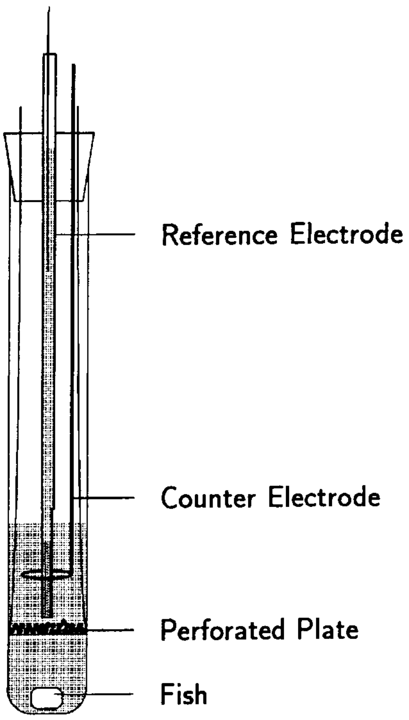

Fig. 5. Test tube cell for fast retrieval of numerous adsorption equilibria data in parallel.

carbon (200 mg) into an oxygen-free 0.1 M KCl solution (10 ml) and determining the immersion potential by holding a platinum wire into the stirred suspension measuring its potential against a reference electrode [27]. In the same manner, the open circuit potentials of activated carbon (200 mg) were determined in given acidic and basic solutions (10 ml 0.1 M KCl solution plus 0 to 5 ml 0.1 M HCl/NaOH).

## 3. Results and discussion

### 3.1. *Potential dependence of surface acidity of activated carbon*

The point of zero charge in 0.1 M KCl solutions was determined as 310 mV vs sat. Ag/AgCl for Norit ROW 0,8 Supra.

The acidic and basic surface groups of activated carbon (e.g., carboxylic, phenolic) exhibit buffer properties (Equations 1, 2):

$$SCO_2H \rightleftharpoons SCO_2^- + H^+ \quad (1)$$

$$S_2C{=}O + H^+ \rightleftharpoons S_2C{=}OH^+ \quad (2)$$

The volume or weight related concentration of acidic with respect. basic surface groups can be determined by titration [28]. The Norit carbon has 0.3 mmol g$^{-1}$ acidic and 0.2 mmol g$^{-1}$ basic groups on its surface.

Also the open circuit potential of the activated carbon changes with pH and vice versa, a change in the potential causes the pH to increase or to decrease due to release or capture of protons into or from the electrolyte in contact with the material. Figure 6 shows the potential dependence on given pH (dashed lines) and the pH dependence with imposed potential (continuous lines). In all cases the mass of activated carbon amounts to 0.125 g equilibrated with 10 ml of 0.1 M KCl solution. The slope of the curve is approximately 60 mV dec.$^{-1}$, as expected for a single proton transfer, proposed by Equations 1 and 2. Reaching a pH of 12 equivalent to 10$^{-2}$ molar base, the buffer capacity of the activated carbon is exhausted, no further increase in pH can be observed on enhancing polarization to cathodic potentials beyond −200 mV vs sat. Ag/AgCl.

An electrical capacity of approximately 100 F g$^{-1}$ can be calculated from a charging cycle for the given activated carbon.

### 3.2. *Adsorption isotherms*

*3.2.1. Adsorption from aqueous electrolytes.* Adsorption isotherms are measured to determine the effect of the potential, the pH value, the type of solvent and the ionic strength of the electrolyte on adsorption/desorption equilibria. Figures 7–12 depict typical isotherms by plotting the adsorbate loading, $q$, given in gram adsorbate per gram activated carbon on the ordinate on the left-hand side and in mol adsorbate per gram activated carbon on the ordinate on the right-hand side against the concentration, $c$. The liquid phase concentration on the abscissa, $c$, is given in g dm$^{-3}$ as well as in mmol dm$^{-3}$. The Freundlich isotherm equation

$$q = kc^n \quad (3)$$

is used for fitting the data (see drawn curves). In all cases, the adsorption equilibria show a strong dependence on the applied potentials.

Figure 7 shows the adsorption isotherms of naphthalenesulfonic acid anions, measured at a buffered pH value of 7 and at −600, 0 and + 600 mV, and compares additionally isotherms obtained at different pH values without buffer. The change in pH without adding a buffer occurs due to the protolytic equilibria discussed in Section 3.1 (Equations 1, 2). Going from pH 7 to pH 12 at −600 mV results in weaker adsorption. The

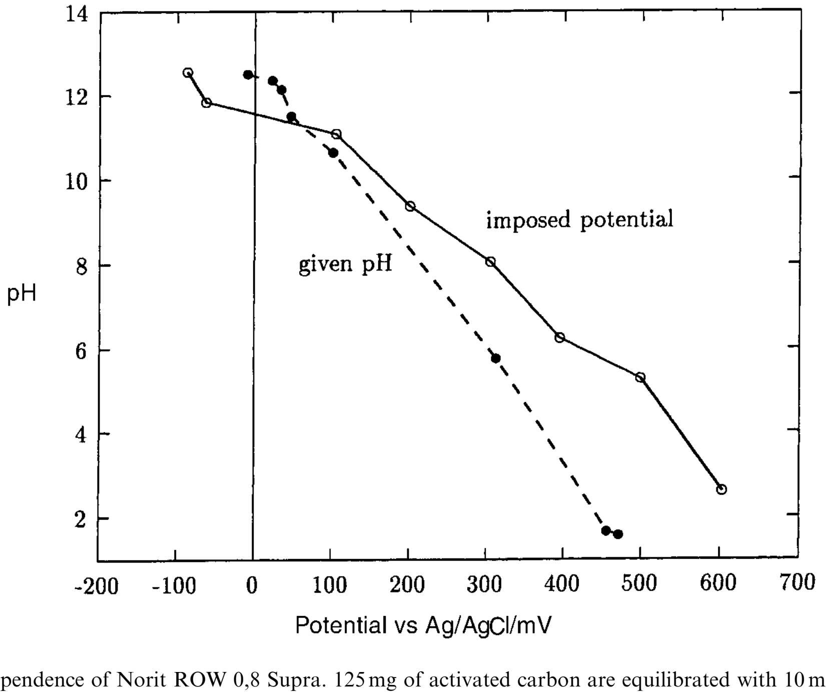

Fig. 6. Potential/pH dependence of Norit ROW 0,8 Supra. 125 mg of activated carbon are equilibrated with 10 ml of 0.1 M KCl solution.

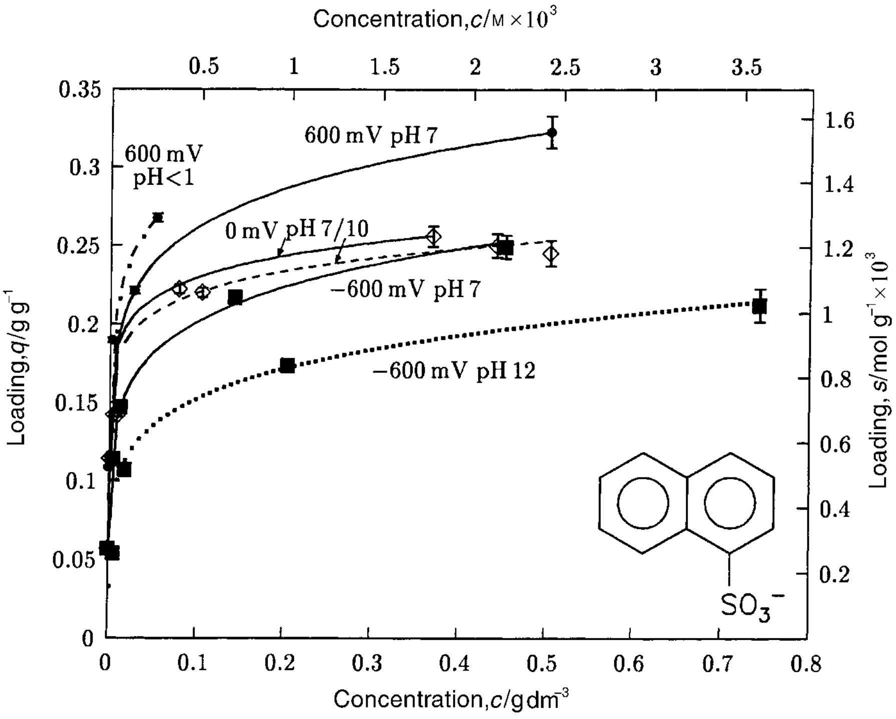

Fig. 7. Adsorption isotherms of naphthalenesulfonic acid anions on activated carbon at different electrode potentials vs sat. Ag/AgCl; electrolyte: 0.1 M KCl; buffer added for pH 1 and pH 7. Drawn lines are calculated according to the model of the Freundlich isotherm.

differences are less pronounced at 0 mV and + 600 mV, but weaker adsorption is always observed at higher pH. The dependence of the adsorption on the applied potential is stronger than on the pH. Additionally, it has to be taken into account that the added buffer also enhances the ionic strength of the electrolyte, an effect discussed below.

As shown in Fig. 8, adsorption of benzyl alcohol, for which adsorption isotherms were measured at −600, 0 and + 600 mV, also exhibits a strong pH dependence at positive potentials. Going to negative potentials, the pH dependence decreases. The influence of the potential on the isotherms is also stronger than that of pH. Going from + 600 to 0 mV the ad-

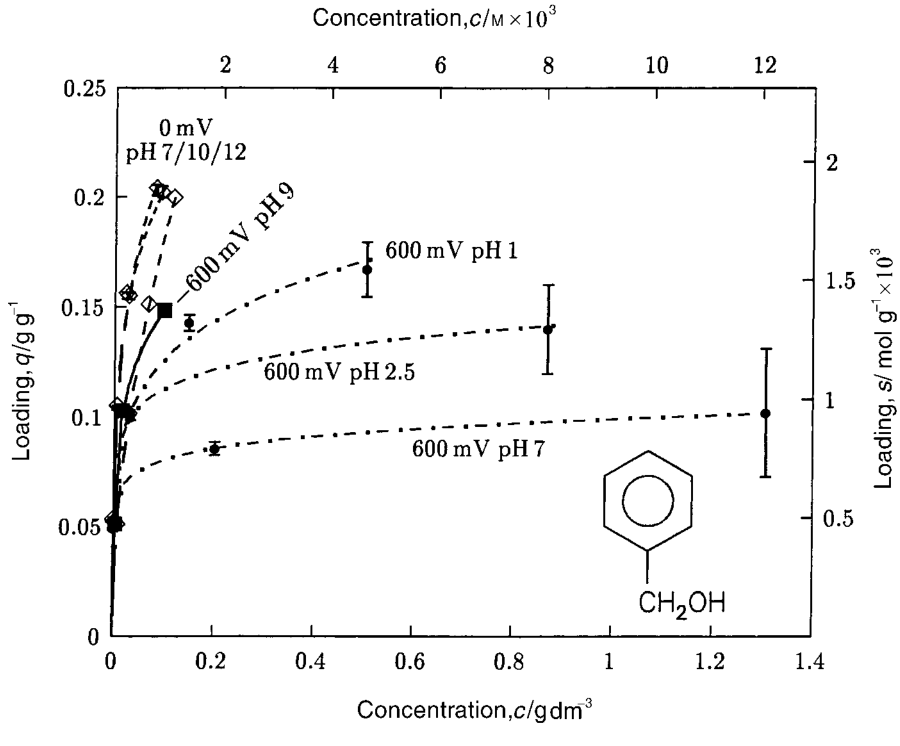

Fig. 8. Adsorption isotherms of benzyl alcohol on activated carbon at different electrode potentials vs sat. Ag/AgCl; electrolyte: 0.1 M KCl; buffer added for pH 1, pH 7, pH 9 and pH 12.

sorption becomes much stronger but at −600 mV the adsorption is again somewhat weaker than at 0 mV.

The situation changes with naphthoate anions. As shown in Fig. 9, the pH value has a stronger effect than the applied potential on the adsorption isotherm. Isotherms below pH 7 cannot be measured due to the poor water solubility of naphthoic acid, which would prevail at pH < 4 due to a $pK_a$ value of 4.17 [29].

*3.2.2. Dependence of adsorption isotherms on ionic strength.* In Fig. 10 adsorption isotherms of naphthalenesulfonic acid anions are shown in differently concentrated KCl solutions. A remarkably weaker adsorption at lower electrolyte concentration is seen. Comparing the 2–2 electrolyte $MgSO_4$ of 0.5 M concentration and ionic strength 2 M with the 1–1 electrolyte KCl of 1 M concentration and ionic strength 1 M it is clear that the ionic strength is not the relevant parameter, rather the chemical and solvation properties of the electrolyte ions also have some influence, since, with $MgSO_4$ at $I = 2$ M and KCl with $I = 1$ M almost indistinguishable adsorption isotherms are observed.

*3.2.3. Adsorption from methanol.* Organic compounds are much weaker adsorbed on activated carbon from organic solvents than from water. In Fig. 11 the dashed/dotted lines represent the adsorption isotherms of the naphthalenesulfonic acid anion in methanol at potentials of 200 mV and −600 mV vs sat. Ag/AgCl; these are much flatter than the respective adsorption isotherms in water.

*3.2.4. Ad/desorption cycles.* Figure 12 depicts the adsorption isotherms of methylquinolinium at +600, +300 and 0 mV vs sat. Ag/AgCl. The potential dependence of methylquinolinium adsorption is clear and, as expected, this cationic species is more strongly adsorbed at more negative than positive potentials.

An adsorption/desorption cycle is also shown in Fig. 12. First, the substance is adsorbed at a potential of 0 mV vs Ag/AgCl, then the potential is switched to +600 mV and the species desorbs. After changing the potential back to 0 mV, the system is ready for the next cycle.

The adsorption capacity of the activated carbon measured for multiple recycling (up to 12 cycles) does not change significantly and might be assumed to be little affected by cycling.

### 3.3. *Discussion*

The negatively charged substances, naphthalenesulfonate and naphthoate, show an absorbability dependence as expected: going from negative to positive potentials, the adsorption becomes stronger due to coulombic interactions between the charged surface and the ions.

The positively charged substance, methylquinolinium, shows a similar behaviour at potentials with opposite sign. Since methylquinolinium is decomposed cathodically at activated carbon below 0 mV vs sat. Ag/AgCl, although at massive carbon or Pt-electrodes a reduction of this cation cannot be observed by cyclic voltammetry, the adsorption isotherm is not defined at $E < 0$ mV.

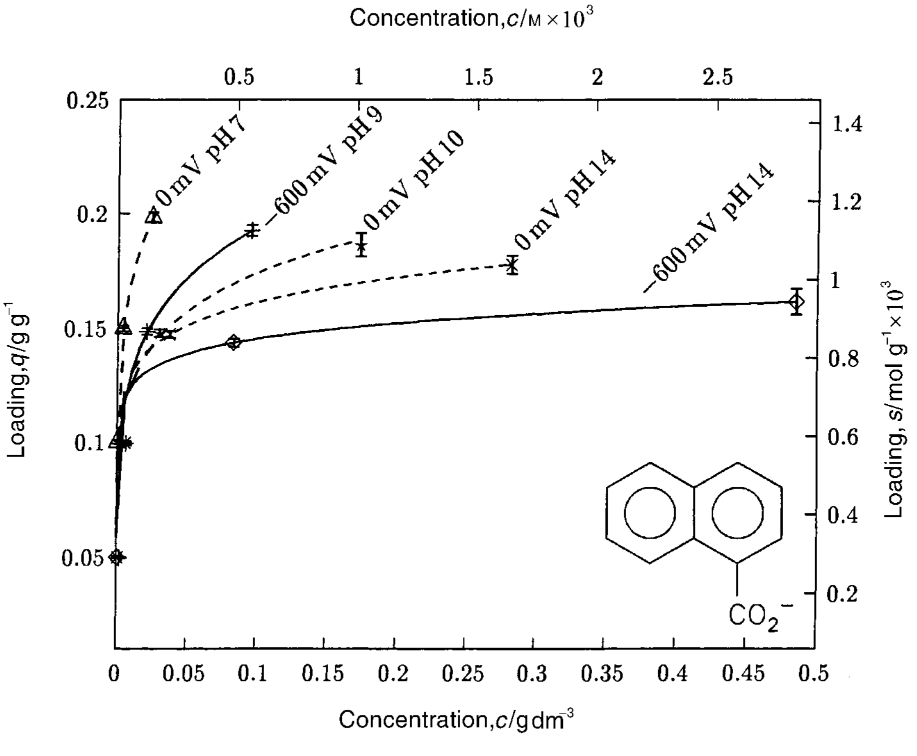

Fig. 9. Adsorption isotherms of naphthoic acid anions on activated carbon at different electrode potentials vs sat. Ag/AgCl; electrolyte: 0.1 M KCl; buffer added for pH 7, pH 9 and pH 14.

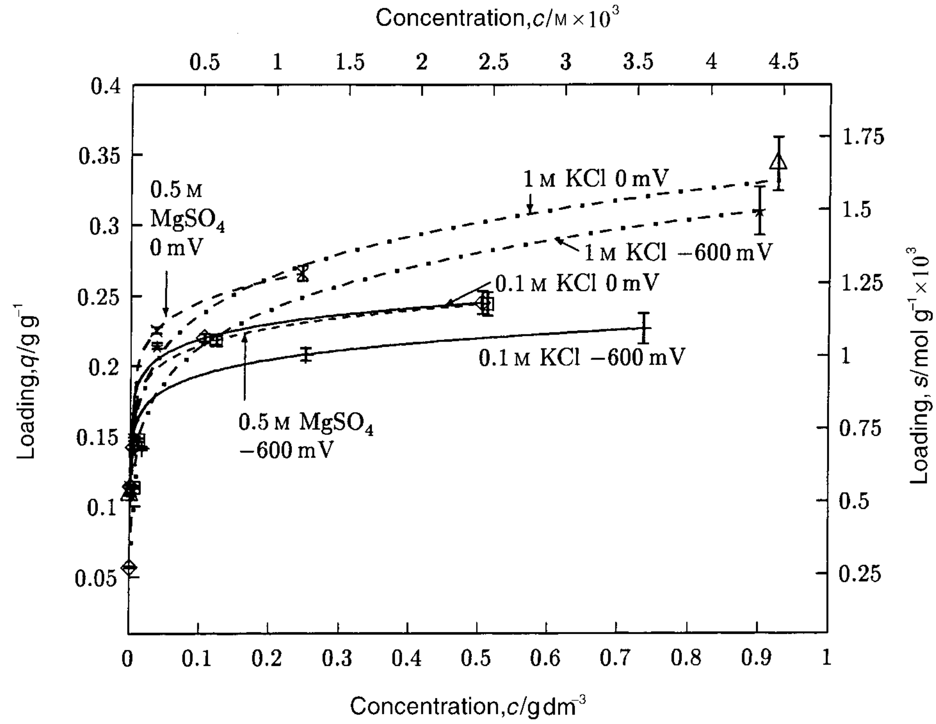

Fig. 10. Adsorption isotherms of naphthalenesulfonic acid anions on activated carbon in 0.1 M KCl (continuous lines), 0.5 M $MgSO_4$ (dashed lines) and 1 M KCl (dashed/dotted lines), electrode potentials vs sat. Ag/AgCl; pH values: pH 10 at 0 mV, pH 12 at 600 mV.

An increase in pH from acidic to basic solutions reduces the adsorbability. As explained in Section 3.1, the equilibrium reaction between solvated hydroxide ions and surface groups in basic solutions leads to an increase in the total amount of negative charge at the surface, which results in an enhanced coulombic repulsion and reduced equilibrium loading of the organic anions.

The shift in the adsorption equilibria, dependent on the electrolyte concentration, can be mainly explained by the salting-out effect, the decrease of water activity due to binding of water molecules by solvation of the electrolyte ions (in particular by the cations).

Figure 13 summarizes the result of this investigation in comparing the influence of the electrode potential on the adsorption equilibrium for the three

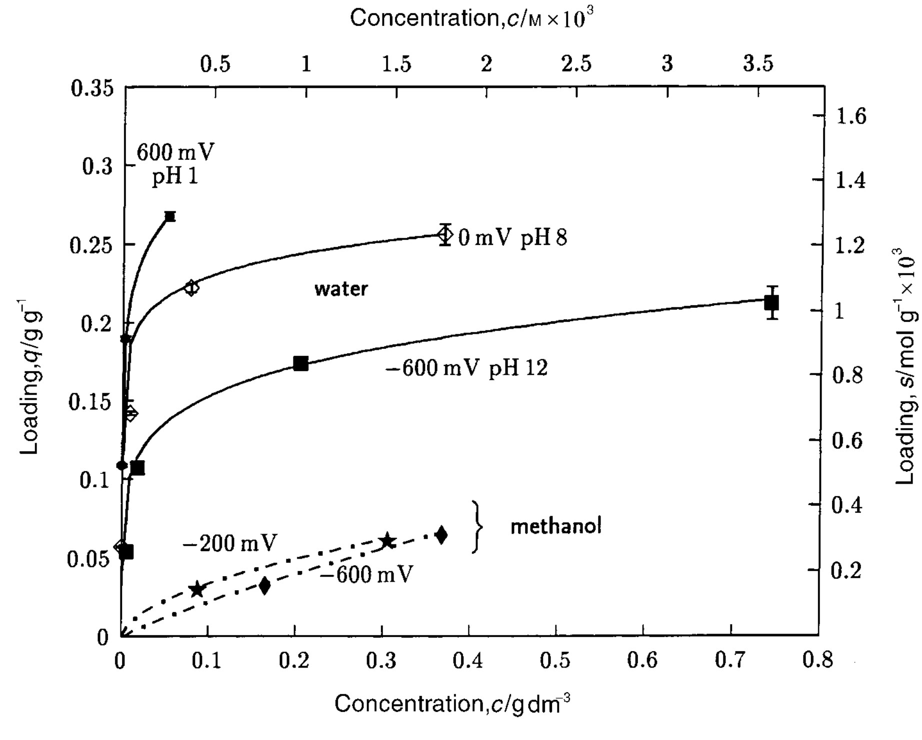

Fig. 11. Adsorption isotherms of naphthalenesulfonic acid anions on activated carbon in aqueous (continuous lines) and methanol (dashed/dotted lines) solution, electrode potentials vs aqueous sat. Ag/AgCl; electrolyte: 0.1 M KCl (0.1 M LiCl in methanol).

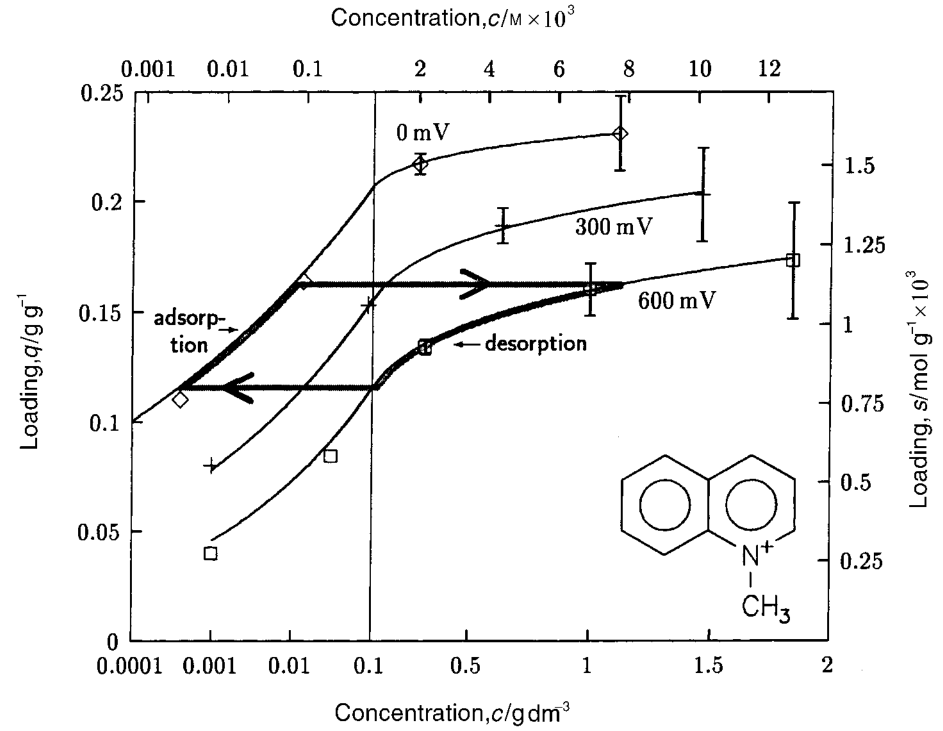

Fig. 12. Adsorption isotherms of methylquinolinium chloride on activated carbon at different electrode potentials vs sat. Ag/AgCl, with an example of an adsorption/desorption cycle; electrolyte: 0.1 M KCl. Schematic demonstration of a potential controlled adsorption/desorption cycle. Note that the concentration scale up to 0.1 g dm$^{-3}$ is logarithmic and above this value is linear. Observe that for a practical application it would be desirable to unload the carbon by desorption to almost zero loading.

differently charged species for selected adsorption isotherms. In this diagram the loading, $q$, of the activated carbon is plotted against the electrode potential at a given adsorbate concentration of $10^{-3}$ M in 0.1 M KCl solution. The loading is highest for uncharged species, benzyl alcohol, which reaches a maximum at approximately 300 mV related to $E_{pzc}$ and decreases at more positive and negative potentials. The influence of the potential, $E$, on the adsorption of the charged species is qualitatively in agreement with expectation according to Fig. 2. But the influence of the potential is much weaker than anticipated from data known for electrosorption on mercury.

The Freundlich exponents, $n$ and $k$, are plotted in Fig. 14 against the potential for adsorption of the four different adsorbates from aqueous 0.1 M KCl solution. Except for the naphthalenesulfonate anion, variation of the exponential, $n$, with potential reflects the variation of the loading, $q$ or $s$, with potential in Fig. 13. Also the correlation of the preexponential factor, $k$, with $E$ in Fig. 14(a) matches that of the

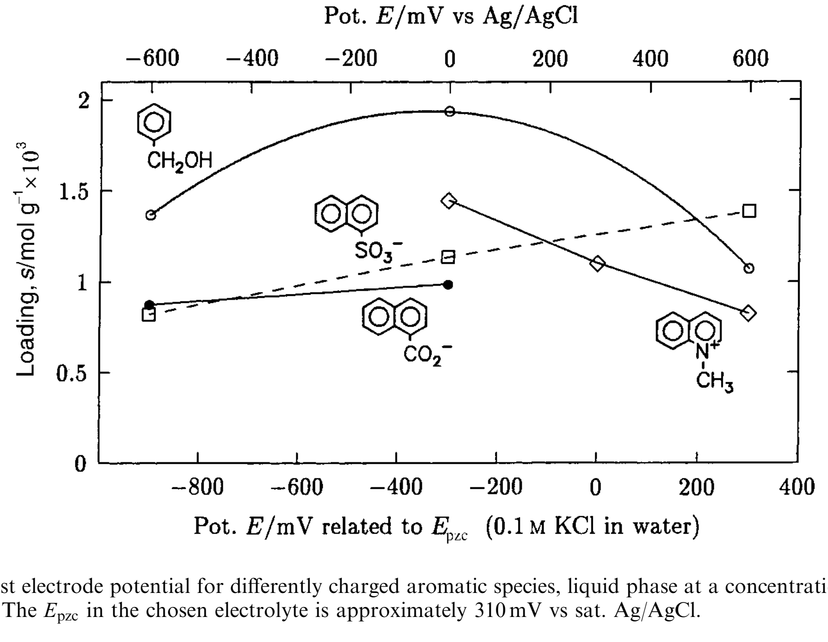

Fig. 13. Loading against electrode potential for differently charged aromatic species, liquid phase at a concentration of $c = 1\,\mu\text{mol dm}^{-3}$; electrolyte: 0.1 M KCl. The $E_{pzc}$ in the chosen electrolyte is approximately 310 mV vs sat. Ag/AgCl.

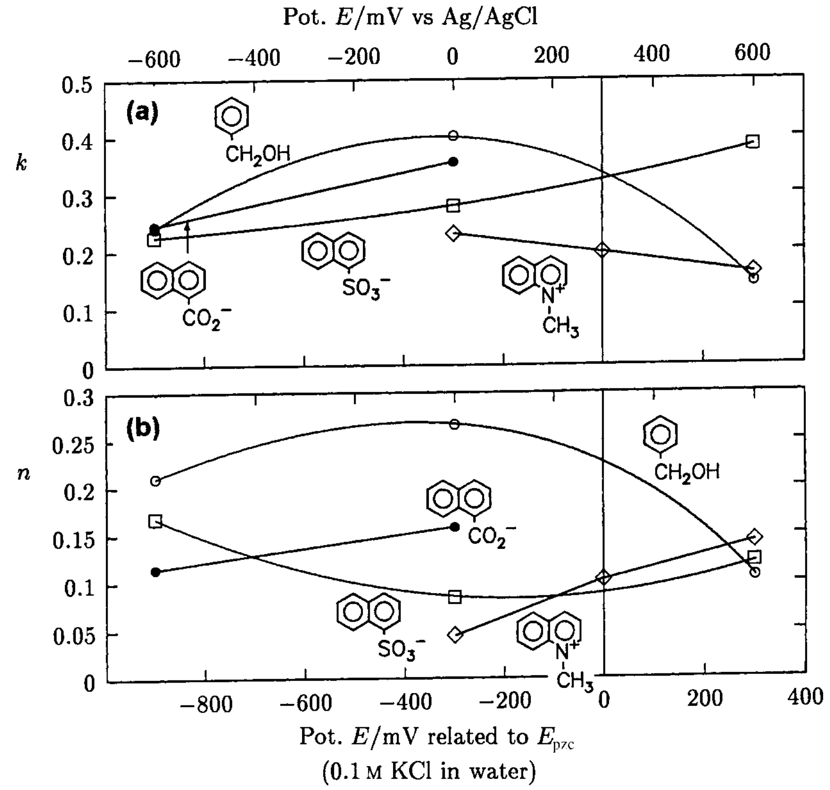

Fig. 14. Potential dependence of Freundlich coefficients, $k$ and $n$, for the adsorption of four different adsorbates from 0.1 M aqueous KCl solution.

loading correlation of Fig. 13. With electrosorption from aqueous solution, a fivefold enhancement of the concentration in one adsorption/desorption cycle is achievable. An improvement beyond this value is possible with countercurrent desorption. The use of the solvent methanol instead of water in the desorption step of an ad-/desorption cycle would allow for a concentration enhancement by a factor of hundred or more, since at a given loading of the adsorbent established in water, for example for $q = 0.1\,\mathrm{g\,g^{-1}}$ (at concentration $c = 0.002\,\mathrm{g\,dm^{-3}}$ and 600 mV) the equilibrium concentration in methanol at −200 mV would be higher than $c = 0.5\,\mathrm{g\,dm^{-3}}$.

## Acknowledgements

The authors are indebted to the Bundesministerium für Wirtschaft for financial support of this project which is financed in the framework of the Arbeitsgemeinschaft industrieller Forschungsvorhaben (AiF-nr. 9752) and is supported by Dechema.

## References

[1] H. Sontheimer, B. R. Frick, J. Fettig, G. Hörner, C. Hubele and G. Zimmer, Adsorptionsverfahren zur Wasserreinigung, DVGW-Forschungsstelle am Engler-Bunte-Institut der Universität Karlsruhe (TH) (1985).

[2] J. Boere (Norit N. V., Amersfoort, NL), Personal communication (1994).

[3] H. Wendt and P. Riemenschneider, *Chem.-Ing.-Tech.* **50** (1978) 250.

[4] K. J. Vetter and J. W. Schultze, *Ber. Bunsenges. Phys. Chem.* **76** (1976) 920.

[5] J. O'M. Bockris and A. K. N. Reddy, 'Modern Electrochemistry', Vols 1 and 2, Plenum Press, New York (1970).

[6] R. C. Alkire and R. S. Eisinger, *J. Electrochem. Soc.* **130** (1983) 85.

[7] R. S. Eisinger and R. C. Alkire, *J. Electroanal. Chem.* **112** (1980) 327.

[8] J. H. Strohl and K. L. Dunlap, *Anal. Chem.* **44** (1972) 2166.

[9] V. V. Khabalov, A. A. Pershko, N. K. Gortshakova and V. Yu. Glushchenko, *Izv. Akad. Nauk SSSR, Ser. Khim.* No. 2 (1984) 263.

[10] P. J. Mayne and R. Shackleton, *J. Appl. Electrochem.* **15** (1985) 745.

[11] J. McGuire, C. F. Dwiggins and P. S. Fedkiw, *ibid.* **15** (1985) 53.

[12] R. M. Narbaitz and J. Cen, *Wat. Res.* **28** (1994) 1771.

[13] V. V. Khabalov, N. P. Morgun, V. L. Zidacevskaya, A. P. Artem'yanov and V. Yu. Glushchenko, *Khim. Tekhnol. Vody* [Engl. trans.] **11** (1989) 27.

[14] E. M. Novikova, K. A. Kazdobin, L. A. Klimenko, Yu. V. Maroresku and V. N. Belyakov, *Ukr. Khim. Zh.* [Engl. trans.] **56** (1990) 75.

[15] K.T. Chue, G. Grevillot and D. Tondeur, in: DECHEMA e.V. (Ed.), Proceedings of the Fourth World Congress Chemical Engineering, Frankfurt/M. (1992) p. 992.

[16] N. Costarramone, S. Hazourli, G. Bonnecaze and M. Astruc, *Environ. Technol.* **15** (1994) 199.

[17] I. G. Lisitskaya, L. P. Lazareva, N. K. Gorchakova, V. V. Khabalov and L. M. Vatrogova, *Khim. Tekhnol. Vody* **12** (1990) 3.

[18] I. A. Tarkovskaya, V. E. Goba, V. Yu. Atamanyuk and T. V. Makhnovskaya, *Khim Tekhnol.* (*Kiev*) **177** (1991) 38.

[19] J. Zabasajja and R. F. Savinell, *AIChE J.* **35** (1989) 755.

[20] E. G. Abramov, *Doklady Chem. Technol.* **313** (1990) 79.

[21] J. O. Besenhard, J. Jakob, P. Moeller and M. Wicher, *DECHEMA Monographien* **121** (1990) 355.

[22] B. E. Reed and S. K. Nonavinakere, *Sep. Sci. Technol.* **27** (1992) 1985.

[23] G. Grevillot, *Adsorption: Science and Technology* (1989) Verlag, p. 193.

[24] B. Kastening, *Ber. Bunsenges. Phys. Chem.* **92** (1988) 1399.

[25] B. Kastening and M. Müller, *J. Electroanal. Chem.* **374** (1994) 159.
[26] A. Schäfer, Dissertation, Tu Darmstadt, (1997).
[27] M. Müller and B. Kastening, *J. Electroanal. Chem.* **374** (1994) 149.
[28] J. S. Mattson and H. B. Mark, 'Activated Carbon: Surface Chemistry and Adsorption from Solution', Marcel Dekker, New York (1971).
[29] R. C. Weast (Ed.), 'CRC Handbook of Chemistry and Physics', 64th edn, CRC Press, Boca Raton, FL (1984).

## Appendix: Adsorption/desorption processes and macrokinetics of adsorption in a bed of activated carbon

As shown by Sontheimer *et al.* [1] and also by our own experiments, the kinetics of electrosorption on granular activated carbon is diffusion controlled and the diffusion into the single particle is the rate determining step. Therefore, reducing the particle size reduces diffusion time and generates steeper breakthrough curves. We observe in the loop (Fig. 3) concentration relaxation times of roughly 4000 s if film diffusion is eliminated by fast convection. Such relaxation times can be calculated from the pellet dimensions (0.8 mm × 3 mm) and the effective diffusion coefficients of order $10^{-6}\,\mathrm{cm^2\,s^{-1}}$. With respect to an application of electrosorption on a technical scale, and taking account of the well known laws of current penetration into porous electrodes, layered absorbers with granular activated carbon and intercalated counter electrodes or stacks of contrapolar activated carbon layers seem to be promising, in which the layer thickness is adjusted to the penetration depth of the charging current associated with the adsorption process. Figure 15 shows the details of two different arrangements, (a) a monopolar and (b) a bipolar adsorber bed.

In both arrangements, the direction of electric current and the flow direction are perpendicular to each other. The small width of the carbon layers (not exceeding 5 cm) is necessary to keep the charging time of the bed short and to provide a uniform potential in the bed.

In Fig. 15(a), polymer fabrics cover the counter electrodes and separate them from the carbon beds. At the counter electrodes, hydrogen or oxygen is evolved, depending on the polarity of the cell. Figure 15(b) shows a bipolar stacked bed. In this case both electrodes are forming adsorber beds. The contrapolar activated carbon beds are separated by a diaphragm.

For a large quantity of substance to be treated electrochemically, case (a) is more suitable, because the current is not limited by capacitive charging. In case (b) no extra energy is consumed at the counter electrode, because both electrode and counter electrode are carbon beds, their double layers being charged with opposite sign. But as long as the bed potentials are kept below a certain threshold beyond which electrochemical conversion occurs, no chlorine evolution or generation of AOX (adsorbable organic halogen compounds) can arise during the treatment of chloride containing waste water.

Instead of granular carbon, activated carbon felt (Actitex company, Levallois, France) can also be used as adsorbent; this offers several advantages: The diameter of its fibres is much smaller than that of activated carbon granules, so the diffusion time in the pores and the adsorption/desorption time is considerably reduced. Also the conductivity of the material is higher than that of a packed carbon bed.

The electrical energy which is consumed by a charge/discharge cycle is obviously not prohibitively large. Electrical energy of $\sim 50\,\mathrm{kWh\,m^{-3}}$ activated carbon is required for charging the electric double layer with a specific capacity of $150\,\mathrm{F\,g^{-1}}$ of activated carbon applying a potential step of $\Delta E = 1.2\,\mathrm{V}$ in one desorption step. For the adsorption/desorption cycle in Fig. 12, 33 kg of adsorbate per $\mathrm{m^3}$ activated carbon can be removed, reducing the concentration of organic substances in the run-off to less than 1 ppm.

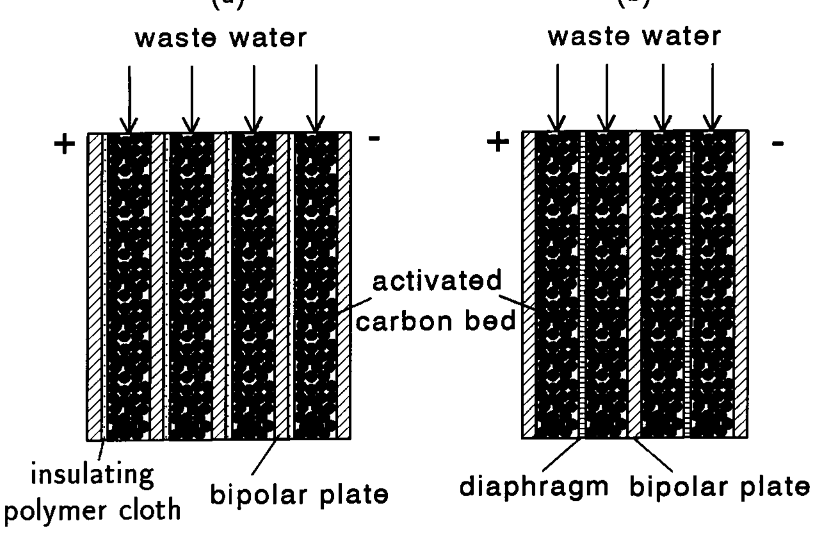

Fig. 15. Arrangement of potential controlled adsorber beds; (a) monopolar, (b) bipolar.